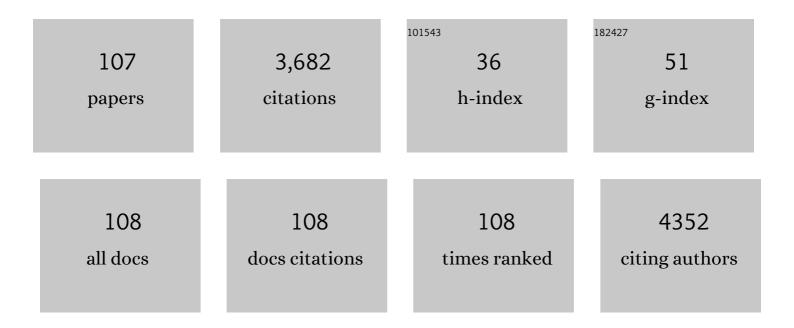


List of Publications by Year in descending order

Source: https://exaly.com/author-pdf/1401173/publications.pdf Version: 2024-02-01



DENC XUE

#	Article	IF	CITATIONS
1	Catalytically Active CoFe ₂ O ₄ Nanoflowers for Augmented Sonodynamic and Chemodynamic Combination Therapy with Elicitation of Robust Immune Response. ACS Nano, 2021, 15, 11953-11969.	14.6	114
2	Biomimetic CoO@AuPt nanozyme responsive to multiple tumor microenvironmental clues for augmenting chemodynamic therapy. Biomaterials, 2020, 257, 120279.	11.4	99
3	ROS-responsive cyclodextrin nanoplatform for combined photodynamic therapy and chemotherapy of cancer. Chinese Chemical Letters, 2021, 32, 162-167.	9.0	98
4	Multifunctional silica nanoparticles as a promising theranostic platform for biomedical applications. Materials Chemistry Frontiers, 2017, 1, 1257-1272.	5.9	85
5	Surface Modification of Poly(dimethylsiloxane) with Polydopamine and Hyaluronic Acid To Enhance Hemocompatibility for Potential Applications in Medical Implants or Devices. ACS Applied Materials & Interfaces, 2017, 9, 33632-33644.	8.0	85
6	Phase-Change Material Packaged within Hollow Copper Sulfide Nanoparticles Carrying Doxorubicin and Chlorin e6 for Fluorescence-Guided Trimodal Therapy of Cancer. ACS Applied Materials & Interfaces, 2019, 11, 417-429.	8.0	84
7	Indocyanine Green-Conjugated Magnetic Prussian Blue Nanoparticles for Synchronous Photothermal/Photodynamic Tumor Therapy. Nano-Micro Letters, 2018, 10, 74.	27.0	81
8	Bioengineered nanogels for cancer immunotherapy. Chemical Society Reviews, 2022, 51, 5136-5174.	38.1	81
9	A concentration gradient generator on a paper-based microfluidic chip coupled with cell culture microarray for high-throughput drug screening. Biomedical Microdevices, 2016, 18, 21.	2.8	77
10	Engineering oxygen-deficient ZrO2-x nanoplatform as therapy-activated "immunogenic cell death (ICD)―inducer to synergize photothermal-augmented sonodynamic tumor elimination in NIR-II biological window. Biomaterials, 2021, 272, 120787.	11.4	77
11	Highly-efficient PVDF adsorptive membrane filtration based on chitosan@CNTs-COOH simultaneous removal of anionic and cationic dyes. Carbohydrate Polymers, 2021, 274, 118664.	10.2	77
12	Prodrugâ€Based Versatile Nanomedicine for Enhancing Cancer Immunotherapy by Increasing Immunogenic Cell Death. Small, 2020, 16, e2000214.	10.0	73
13	Highly Porous Silk Fibroin Scaffold Packed in PEGDA/Sucrose Microneedles for Controllable Transdermal Drug Delivery. Biomacromolecules, 2019, 20, 1334-1345.	5.4	69
14	Biomineralization-inspired Crystallization of Manganese Oxide on Silk Fibroin Nanoparticles for <i>in vivo</i> MR/fluorescence Imaging-assisted Tri-modal Therapy of Cancer. Theranostics, 2019, 9, 6314-6333.	10.0	67
15	Bioresponsive immune-booster-based prodrug nanogel for cancer immunotherapy. Acta Pharmaceutica Sinica B, 2022, 12, 451-466.	12.0	66
16	Indocyanine green-modified hollow mesoporous Prussian blue nanoparticles loading doxorubicin for fluorescence-guided tri-modal combination therapy of cancer. Nanoscale, 2019, 11, 5717-5731.	5.6	64
17	Light-activated oxygen self-supplied starving therapy in near-infrared (NIR) window and adjuvant hyperthermia-induced tumor ablation with an augmented sensitivity. Biomaterials, 2020, 234, 119771.	11.4	59
18	Light-activatable Chlorin e6 (Ce6)-imbedded erythrocyte membrane vesicles camouflaged Prussian blue nanoparticles for synergistic photothermal and photodynamic therapies of cancer. Biomaterials Science, 2018, 6, 2881-2895.	5.4	56

#	Article	IF	CITATIONS
19	Smart Unimolecular Micelle-Based Polyprodrug with Dual-Redox Stimuli Response for Tumor Microenvironment: Enhanced in Vivo Delivery Efficiency and Tumor Penetration. ACS Applied Materials & Interfaces, 2019, 11, 36130-36140.	8.0	56
20	Calcium-carbonate packaging magnetic polydopamine nanoparticles loaded with indocyanine green for near-infrared induced photothermal/photodynamic therapy. Acta Biomaterialia, 2018, 81, 242-255.	8.3	53
21	Responsive agarose hydrogel incorporated with natural humic acid and MnO ₂ nanoparticles for effective relief of tumor hypoxia and enhanced photo-induced tumor therapy. Biomaterials Science, 2020, 8, 353-369.	5.4	53
22	Tumor microenvironment responsive biomimetic copper peroxide nanoreactors for drug delivery and enhanced chemodynamic therapy. Chemical Engineering Journal, 2021, 416, 129037.	12.7	53
23	PEGylated polydopamine-coated magnetic nanoparticles for combined targeted chemotherapy and photothermal ablation of tumour cells. Colloids and Surfaces B: Biointerfaces, 2017, 160, 11-21.	5.0	51
24	Redox-Sensitive Citronellol–Cabazitaxel Conjugate: Maintained in Vitro Cytotoxicity and Self-Assembled as Multifunctional Nanomedicine. Bioconjugate Chemistry, 2016, 27, 1360-1372.	3.6	50
25	Cylindrical polymer brushes-anisotropic unimolecular micelle drug delivery system for enhancing the effectiveness of chemotherapy. Bioactive Materials, 2021, 6, 2894-2904.	15.6	48
26	An in-vitro study of enzyme-responsive Prussian blue nanoparticles for combined tumor chemotherapy and photothermal therapy. Colloids and Surfaces B: Biointerfaces, 2015, 125, 277-283.	5.0	47
27	pH-Responsive unimolecular micelles based on amphiphilic star-like copolymers with high drug loading for effective drug delivery and cellular imaging. Journal of Materials Chemistry B, 2017, 5, 6847-6859.	5.8	44
28	Starburst Diblock Polyprodrugs: Reduction-Responsive Unimolecular Micelles with High Drug Loading and Robust Micellar Stability for Programmed Delivery of Anticancer Drugs. Biomacromolecules, 2019, 20, 1190-1202.	5.4	44
29	Supramolecular Tadalafil Nanovaccine for Cancer Immunotherapy by Alleviating Myeloidâ€Derived Suppressor Cells and Heightening Immunogenicity. Small Methods, 2021, 5, e2100115.	8.6	44
30	Rapidly cell-penetrating and reductive milieu-responsive nanoaggregates assembled from an amphiphilic folate-camptothecin prodrug for enhanced drug delivery and controlled release. Biomaterials Science, 2017, 5, 444-454.	5.4	43
31	Reduction stimuli-responsive unimolecular polymeric prodrug based on amphiphilic dextran-framework for antitumor drug delivery. Carbohydrate Polymers, 2018, 182, 235-244.	10.2	42
32	pH-responsive polymeric micelles based on poly(ethyleneglycol)-b-poly(2-(diisopropylamino) ethyl) Tj ETQqO 0 0 Colloid and Interface Science, 2017, 490, 511-519.	rgBT /Ove 9.4	rlock 10 Tf 50 41
33	Injectable and Natural Humic Acid/Agarose Hybrid Hydrogel for Localized Light-Driven Photothermal Ablation and Chemotherapy of Cancer. ACS Biomaterials Science and Engineering, 2018, 4, 4266-4277.	5.2	41
34	Blood sampling using microneedles as a minimally invasive platform for biomedical diagnostics. Applied Materials Today, 2018, 13, 144-157.	4.3	41
35	Methotrexate-based amphiphilic prodrug nanoaggregates for co-administration of multiple therapeutics and synergistic cancer therapy. Acta Biomaterialia, 2018, 77, 228-239.	8.3	41
36	Flexible PEGDA-based microneedle patches with detachable PVP–CD arrowheads for transdermal drug delivery. RSC Advances, 2015, 5, 75204-75209.	3.6	40

#	Article	IF	CITATIONS
37	Glutathione-Responsive Multifunctional "Trojan Horse―Nanogel as a Nanotheranostic for Combined Chemotherapy and Photodynamic Anticancer Therapy. ACS Applied Materials & Interfaces, 2020, 12, 50896-50908.	8.0	37
38	Novel Oxygen-Deficient Zirconia (ZrO _{2–<i>x</i>}) for Fluorescence/Photoacoustic Imaging-Guided Photothermal/Photodynamic Therapy for Cancer. ACS Applied Materials & Interfaces, 2019, 11, 41127-41139.	8.0	35
39	Reduction-Responsive Chemo-Capsule-Based Prodrug Nanogel for Synergistic Treatment of Tumor Chemotherapy. ACS Applied Materials & Interfaces, 2021, 13, 8940-8951.	8.0	35
40	Suppression of NRF2–ARE activity sensitizes chemotherapeutic agent-induced cytotoxicity in human acute monocytic leukemia cells. Toxicology and Applied Pharmacology, 2016, 292, 1-7.	2.8	34
41	Reduction-active polymeric prodrug micelles based on α-cyclodextrin polyrotaxanes for triggered drug release and enhanced cancer therapy. Carbohydrate Polymers, 2018, 193, 153-162.	10.2	34
42	PEGylated magnetic Prussian blue nanoparticles as a multifunctional therapeutic agent for combined targeted photothermal ablation and pH-triggered chemotherapy of tumour cells. Journal of Colloid and Interface Science, 2018, 509, 384-394.	9.4	34
43	PEGylated Polydopamine Nanoparticles Incorporated with Indocyanine Green and Doxorubicin for Magnetically Guided Multimodal Cancer Therapy Triggered by Near-Infrared Light. ACS Applied Nano Materials, 2018, 1, 325-336.	5.0	34
44	Polydopamine (PDA)-activated cobalt sulfide nanospheres responsive to tumor microenvironment (TME) for chemotherapeutic-enhanced photothermal therapy. Chinese Chemical Letters, 2021, 32, 1055-1060.	9.0	34
45	Acid-Activatable Theranostic Unimolecular Micelles Composed of Amphiphilic Star-like Polymeric Prodrug with High Drug Loading for Enhanced Cancer Therapy. Molecular Pharmaceutics, 2017, 14, 4032-4041.	4.6	33
46	Disassembly of amphiphilic small molecular prodrug with fluorescence switch induced by pH and folic acid receptors for targeted delivery and controlled release. Colloids and Surfaces B: Biointerfaces, 2017, 150, 50-58.	5.0	32
47	PEGDA/PVP Microneedles with Tailorable Matrix Constitutions for Controllable Transdermal Drug Delivery. Macromolecular Materials and Engineering, 2018, 303, 1800233.	3.6	31
48	A HMCuS@MnO ₂ nanocomplex responsive to multiple tumor environmental clues for photoacoustic/fluorescence/magnetic resonance trimodal imaging-guided and enhanced photothermal/photodynamic therapy. Nanoscale, 2020, 12, 12508-12521.	5.6	31
49	Mitochondria-Specific Anticancer Drug Delivery Based on Reduction-Activated Polyprodrug for Enhancing the Therapeutic Effect of Breast Cancer Chemotherapy. ACS Applied Materials & Interfaces, 2019, 11, 29330-29340.	8.0	30
50	Multifunctional SGQDs-CORM@HA nanosheets for bacterial eradication through cascade-activated "nanoknife―effect and photodynamic/CO gas therapy. Biomaterials, 2021, 277, 121084.	11.4	30
51	Bimetallic PdPt-based nanocatalysts for Photothermal-Augmented tumor starvation and sonodynamic therapy in NIR-II biowindow assisted by an oxygen Self-Supply strategy. Chemical Engineering Journal, 2022, 435, 135085.	12.7	30
52	Transdermal delivery of therapeutics through dissolvable gelatin/sucrose films coated on PEGDA microneedle arrays with improved skin permeability. Journal of Materials Chemistry B, 2019, 7, 7515-7524.	5.8	29
53	Constructing high effective nano-Mn3(PO4)2-chitosan in situ electrochemical detection interface for superoxide anions released from living cell. Biosensors and Bioelectronics, 2019, 133, 133-140.	10.1	29
54	A bottlebrush-architectured dextran polyprodrug as an acidity-responsive vector for enhanced chemotherapy efficiency. Biomaterials Science, 2020, 8, 473-484.	5.4	29

#	Article	IF	CITATIONS
55	Ultrasound (US)-activated redox dyshomeostasis therapy reinforced by immunogenic cell death (ICD) through a mitochondrial targeting liposomal nanosystem. Theranostics, 2021, 11, 9470-9491.	10.0	29
56	Protein Covalently Conjugated SU-8 Surface for the Enhancement of Mesenchymal Stem Cell Adhesion and Proliferation. Langmuir, 2014, 30, 3110-3117.	3.5	27
57	Microfluidic synthesis of monodisperse PEGDA microbeads for sustained release of 5-fluorouracil. Microfluidics and Nanofluidics, 2015, 18, 333-342.	2.2	27
58	Polydopamineâ€collagen complex to enhance the biocompatibility of polydimethylsiloxane substrates for sustaining longâ€term culture of L929 fibroblasts and tendon stem cells. Journal of Biomedical Materials Research - Part A, 2018, 106, 408-418.	4.0	27
59	A simple technique of constructing nano-roughened polydimethylsiloxane surface to enhance mesenchymal stem cell adhesion and proliferation. Microfluidics and Nanofluidics, 2018, 22, 1.	2.2	27
60	Codelivery of doxorubicin and camptothecin by dual-responsive unimolecular micelle-based β-cyclodextrin for enhanced chemotherapy. Colloids and Surfaces B: Biointerfaces, 2019, 183, 110428.	5.0	27
61	PEGylated mesoporous Bi2S3 nanostars loaded with chlorin e6 and doxorubicin for fluorescence/CT imaging-guided multimodal therapy of cancer. Nanomedicine: Nanotechnology, Biology, and Medicine, 2019, 17, 1-12.	3.3	27
62	Magnetic Prussian blue nanoparticles for combined enzyme-responsive drug release and photothermal therapy. RSC Advances, 2015, 5, 28401-28409.	3.6	26
63	Acid-active supramolecular anticancer nanoparticles based on cyclodextrin polyrotaxanes damaging both mitochondria and nuclei of tumor cells. Biomaterials Science, 2018, 6, 3126-3138.	5.4	25
64	Facile engineering of silk fibroin capped AuPt bimetallic nanozyme responsive to tumor microenvironmental factors for enhanced nanocatalytic therapy. Theranostics, 2021, 11, 107-116.	10.0	25
65	Drug-eluting microneedles for self-administered treatment of keloids. Technology, 2014, 02, 144-152.	1.4	24
66	Stimuli responsive PEGylated bismuth selenide hollow nanocapsules for fluorescence/CT imaging and light-driven multimodal tumor therapy. Biomaterials Science, 2019, 7, 3025-3040.	5.4	24
67	Electrochemical―and Fluorescentâ€Mediated Signal Amplifications for Rapid Detection of Lowâ€Abundance Circulating Tumor Cells on a Paperâ€Based Microfluidic Immunodevice. ChemElectroChem, 2014, 1, 722-727.	3.4	23
68	Rational design of oxygen deficient TiO _{2â^'x} nanoparticles conjugated with chlorin e6 (Ce6) for photoacoustic imaging-guided photothermal/photodynamic dual therapy of cancer. Nanoscale, 2020, 12, 1707-1718.	5.6	23
69	Functional magnetic Prussian blue nanoparticles for enhanced gene transfection and photothermal ablation of tumor cells. Journal of Materials Chemistry B, 2016, 4, 4717-4725.	5.8	22
70	Intradermal administration of green synthesized nanosilver (NS) through film-coated PEGDA microneedles for potential antibacterial applications. Biomaterials Science, 2021, 9, 2244-2254.	5.4	21
71	Water-soluble fluorescent unimolecular micelles: ultra-small size, tunable fluorescence emission from the visible to NIR region and enhanced biocompatibility for <i>in vitro</i> and <i>in vivo</i> bioimaging. Chemical Communications, 2018, 54, 6252-6255.	4.1	20
72	Microenvironment-responsive chemotherapeutic nanogels for enhancing tumor therapy via DNA damage and glutathione consumption. Chinese Chemical Letters, 2022, 33, 4197-4202.	9.0	20

#	Article	IF	CITATIONS
73	Active targeting redox-responsive mannosylated prodrug nanocolloids promote tumor recognition and cell internalization for enhanced colon cancer chemotherapy. Acta Biomaterialia, 2022, 147, 299-313.	8.3	20
74	Highly efficient capture and harvest of circulating tumor cells on a microfluidic chip integrated with herringbone and micropost arrays. Biomedical Microdevices, 2015, 17, 39.	2.8	19
75	Enhanced Tumor Penetration and Chemotherapy Efficiency by Covalent Self-Assembled Nanomicelle Responsive to Tumor Microenvironment. Biomacromolecules, 2019, 20, 2637-2648.	5.4	19
76	Acidic TMEâ€Responsive Nanoâ€Bi ₂ Se ₃ @MnCaP as a NIRâ€IIâ€Triggered Free Radical Generator for Hypoxiaâ€Irrelevant Phototherapy with High Specificity and Immunogenicity. Small, 2022, 18, e2104302.	10.0	19
77	BC@DNA-Mn ₃ (PO ₄) ₂ Nanozyme for Real-Time Detection of Superoxide from Living Cells. Analytical Chemistry, 2020, 92, 15927-15935.	6.5	18
78	Acid-Sensitive Supramolecular Nanoassemblies with Multivalent Interaction: Effective Tumor Retention and Deep Intratumor Infiltration. ACS Applied Materials & Interfaces, 2021, 13, 37680-37692.	8.0	18
79	Silk fibroin-capped metal-organic framework for tumor-specific redox dyshomeostasis treatment synergized by deoxygenation-driven chemotherapy. Acta Biomaterialia, 2022, 138, 545-560.	8.3	18
80	Threeâ€dimensional microfluidic chip with twinâ€layer herringbone structure for high efficient tumor cell capture and release via antibodyâ€conjugated magnetic microbeads. Electrophoresis, 2018, 39, 1452-1459.	2.4	17
81	Engineering Eu3+-incorporated MoS2 nanoflowers toward efficient photothermal/photodynamic combination therapy of breast cancer. Applied Surface Science, 2021, 552, 149498.	6.1	17
82	Isolation and elution of Hep3B circulating tumor cells using a dual-functional herringbone chip. Microfluidics and Nanofluidics, 2014, 16, 605-612.	2.2	16
83	Irinotecan delivery by unimolecular micelles composed of reduction-responsive star-like polymeric prodrug with high drug loading for enhanced cancer therapy. Colloids and Surfaces B: Biointerfaces, 2018, 170, 488-496.	5.0	16
84	Engineering silk sericin decorated zeolitic imidazolate framework-8 nanoplatform to enhance chemotherapy. Colloids and Surfaces B: Biointerfaces, 2021, 200, 111594.	5.0	16
85	Persistence of increasing vegetation gross primary production under the interactions of climate change and land use changes in Northwest China. Science of the Total Environment, 2022, 834, 155086.	8.0	16
86	Facile synthesis of hollow mesoporous nickel sulfide nanoparticles for highly efficient combinatorial photothermal–chemotherapy of cancer. Journal of Materials Chemistry B, 2020, 8, 7766-7776.	5.8	15
87	Polyamino acid calcified nanohybrids induce immunogenic cell death for augmented chemotherapy and chemo-photodynamic synergistic therapy. Theranostics, 2021, 11, 9652-9666.	10.0	15
88	A platinum nanourchin-based multi-enzymatic platform to disrupt mitochondrial function assisted by modulating the intracellular H2O2 homeostasis. Biomaterials, 2022, 286, 121572.	11.4	15
89	Enantioselective synthesis of chiral multicyclic γ-lactones <i>via</i> dynamic kinetic resolution of racemic γ-keto carboxylic acids. Organic Chemistry Frontiers, 2020, 7, 104-108.	4.5	11
90	The genotoxic potential of mixed nitrosamines in drinking water involves oxidative stress and Nrf2 activation. Journal of Hazardous Materials, 2022, 426, 128010.	12.4	11

#	Article	IF	CITATIONS
91	Improving the carrier stability and drug loading of unimolecular micelle-based nanotherapeutics for acid-activated drug delivery and enhanced antitumor therapy. Journal of Materials Chemistry B, 2018, 6, 5549-5561.	5.8	10
92	MnO ₂ -capped silk fibroin (SF) nanoparticles with chlorin e6 (Ce6) encapsulation for augmented photo-driven therapy by modulating the tumor microenvironment. Journal of Materials Chemistry B, 2021, 9, 3677-3688.	5.8	10
93	Hydrophilic ionic-liquid grafted poly(vinylidene fluoride) membranes with excellent cationic dye and oil–water emulsion removal performance. Journal of Materials Science, 2022, 57, 4876-4894.	3.7	10
94	Highly cell-penetrating and ultra-pH-responsive nanoplatform for controlled drug release and enhanced tumor therapy. Colloids and Surfaces B: Biointerfaces, 2017, 159, 484-492.	5.0	9
95	Reactive oxygen species-activatable camptothecin polyprodrug based dextran enhances chemotherapy efficacy by damaging mitochondria. Journal of Materials Chemistry B, 2020, 8, 1245-1255.	5.8	9
96	The Systematic Evaluation of Physicochemical and Biological Properties In Vitro and In Vivo for Natural Silk Fibroin Nanoparticles. Advanced Fiber Materials, 2022, 4, 1141-1152.	16.1	9
97	Isolation and retrieval of circulating tumor cells on a microchip with double parallel layers of herringbone structure. Microfluidics and Nanofluidics, 2016, 20, 1.	2.2	8
98	The synthesis of two-dimensional Bi ₂ Te ₃ @SiO ₂ core–shell nanosheets for fluorescence/photoacoustic/infrared (FL/PA/IR) tri-modal imaging-guided photothermal/photodynamic combination therapy. Biomaterials Science, 2020, 8, 5874-5887.	5.4	7
99	Silk Sericin-Based Nanoparticle as the Photosensitizer Chlorin e6 Carrier for Enhanced Cancer Photodynamic Therapy. ACS Sustainable Chemistry and Engineering, 2021, 9, 3213-3222.	6.7	7
100	Development and prospects of microfluidic platforms for sperm inspection. Analytical Methods, 2019, 11, 4547-4560.	2.7	6
101	Co-delivery of chlorin e6 and doxorubicin using PEGylated hollow nanocapsules for â€~all-in-one' tumor theranostics. Nanomedicine, 2019, 14, 2273-2292.	3.3	6
102	Rapid prototyping of Nanoroughened polydimethylsiloxane surfaces for the enhancement of immunomagnetic isolation and recovery of rare tumor cells. Biomedical Microdevices, 2019, 21, 58.	2.8	6
103	In vitro degradation behavior and biocompatibility of Mg–5.8 Zn–2.0 Yb–0.5 Zr alloy during aging treatment. Materials Letters, 2021, 282, 128682.	2.6	6
104	A paper-based photothermal array using Parafilm to analyze hyperthermia response of tumour cells under local gradient temperature. Biomedical Microdevices, 2018, 20, 68.	2.8	5
105	Mercury Chloride Impacts on the Development of Erythrocytes and Megakaryocytes in Mice. Toxics, 2021, 9, 252.	3.7	5
106	Involvement of O2·â~ release in zearalenone-induced hormesis of intestinal porcine enterocytes: An electrochemical sensor-based analysis. Bioelectrochemistry, 2022, 144, 108049.	4.6	2
107	Cadmium suppresses bone marrow thrombopoietin production and impairs megakaryocytopoiesis in mice. Toxicological Sciences, 2022, , .	3.1	2